Journal of Computer Science and Electrical Engineering
Print ISSN: 2663-1938
Online ISSN: 2663-1946
DOI: https://doi.org/10.61784/jcsee3117

LOW-CARBON OPTIMIZATION SCHEDULING STRATEGY FOR INTEGRATED ENERGY SYSTEM CONSIDERING GAS AND THERMAL INERTIA

WenJin Zhang[1*], Geigeicao Qiao[2], Yu Li[1], Qi Chen[1], Jian Yan[1]
[1]*State Grid Gansu Electric Power Company Jinchang Power Supply Company, Jinchang 737100, Gansu, China.*
[2]*Datang Xinjiang Power Generation Co., Ltd. Southern Xinjiang Branch, Wulumuqi 830000, Xinjiang, China.*
[*]*Corresponding Author: WenJin Zhang*

Abstract: With the increasing global emphasis on low-carbon development, integrated energy systems (IES) plays a pivotal role in optimizing energy utilization and reducing carbon emissions. Gas-thermal inertia refers to the energy storage and release characteristics exhibited by gas and thermal energy during transmission and conversion processes. This not only affects the dynamic balance of energy but also poses higher requirements for scheduling optimization.Meanwhile, carbon trading and green certificate trading mechanisms serve as crucial tools for balancing environmental protection and economic benefits. This paper establishes an IES low-carbon economic dispatch model that considers gas-heat inertia, and employs an improved particle swarm optimization algorithm for solving it.Finally, taking a power system in a certain region with a high proportion of renewable energy as a case study, the results show that operating the power system considering gas-thermal inertia can significantly improve the operational economy of the system, optimize the electricity prices in the power market, and enhance the earnings from green certificates and carbon trading.
Keywords: Carbon trading; Green certificate; Power system; Gas and Thermal Inertia

1 INTRODUCTION

In recent years, energy and environmental issues have become increasingly pressing. To achieve the "dual carbon" goals, there is an urgent need to optimize and adjust the energy structure, improve energy efficiency, and promote the widespread application of renewable energy [1]. Increasing the share of new energy in the electricity spot market is one of the main pathways to achieve renewable energy accommodation [2]. The effective coupling of green certificate trading (GCT), carbon trading, and electricity market trading is of great significance for enhancing the utilization rate of renewable energy and reducing carbon emissions in power systems [3].

To date, extensive research has been conducted on the trading mechanisms of electricity markets. Reference proposed an optimization strategy for power market involving multiple entities such as power generators [4], established an optimization model for the electricity-heat integrated energy market, rationally determined market electricity prices, improved the utilization rate of renewable energy, and enhanced social welfare costs. Reference [5], considering the impact of load output uncertainty and based on multi-time scale theory, established an optimal dispatch model for power systems participating in the electricity market under existing market rules, enabling real-time tracking of electricity market price transactions and reducing system energy costs. Reference investigated the optimal configuration problem involving cloud electricity storage and cloud heat storage technologies in the electricity market [6], optimizing users' electricity and heat demands to reduce system costs. Reference introduced an electricity market trading system to construct an optimization model for cooperative user operation incorporating carbon emission reduction strategies [7], balancing individual and collective interests to promote the economic operation of the system. However, the models proposed in the aforementioned studies did not consider the low-carbon operation of power systems. Conversely, carbon trading and green certificate trading mechanisms are crucial for the low-carbon operation of multi-energy power systems and have become key measures for reducing system carbon emissions.

With the development of carbon emissions trading (CET) and green certificate mechanisms, the energy inertia issues of various subsystems within IES have garnered widespread attention. In the context of achieving low-carbon objectives, effectively coordinating the energy inertia of the power grid, gas network, and heating network has become critical. Reference analyzed the impact of electric thermal storage boilers on thermal inertia during the energy conversion process [8]. Reference discussed the effect of heating network characteristics on system ultra-short-term scheduling and proposed a formula based on the scheduling period and pipeline length to determine the transient and steady-state characteristics of the heating network [9]. Reference investigated the positive role of pipeline storage in IES demand response and optimal dispatch, achieving favorable results [10]. Reference pointed out that natural gas pipelines possess the characteristic of buffering energy fluctuations [11], effectively harnessing the potential of the natural gas system and enhancing system flexibility. Reference employed an electro-steady state and gas-transient state model, incorporating the natural gas pipeline storage model as a constraint into IES optimal dispatch. [12] Reference elucidated the interaction mechanism between electricity and gas systems [13], demonstrating the positive impact of natural gas pipeline storage on improving IES flexibility.

Although the aforementioned studies have proposed flexibility enhancement schemes in areas such as demand response and pipeline storage, research on the optimal dispatch of IES clusters within the electricity market environment remains insufficient. Therefore, addressing the limitations of the existing single electricity market trading model and low-carbon dispatch frameworks, this paper proposes an optimal dispatch strategy for multi-energy entities in power systems considering gas-thermal inertia. Finally, four different scenarios are established, and a case study of a power system in a certain region with a high proportion of wind and solar new energy is conducted to verify the feasibility and effectiveness of the proposed strategy.

2 CARBON-GREEN CERTIFICATE TRADING MECHANISM

2.1 Carbon Trading Model

In the carbon trading market, a tiered pricing mechanism is implemented to mitigate system carbon emissions. This approach segments the deviation between actual emissions and the initial allowance into several intervals, thereby enabling a detailed examination of how emission levels correlate with allowance shortfalls or surpluses. The ladder-type carbon trading cost C_1 is shown in the following formula.

$$\min C_1 = \begin{cases} -C_c(2+3C_\mu)l + C_c(1+3C_\mu)(\Delta E_{CO_2} + 2l), \\ \Delta E_{CO_2} \le -2l \\ -C_c(1+C_\mu)l + c(1+2C_\mu)(\Delta E_{CO_2} + l), \\ -2l \le \Delta E_{CO_2} \le -l \\ C_c(1+C_\mu)\Delta E_{CO_2}, \ -l \le \Delta E_{CO_2} \le 0 \\ C_c\Delta E_{CO_2}, \ 0 \le \Delta E_{CO_2} \le l \\ C_c l + C_c(1+C_\beta)(\Delta E_{CO_2} - l), \\ l \le \Delta E_{CO_2} \le 2l \\ C_c(2+C_\beta)l + C_c(1+2C_\beta)(\Delta E_{CO_2} - 2l), \\ 2l \le \Delta E_{CO_2} \end{cases} \tag{1}$$

$$\Delta E_{CO_2} = E^t_{CO_2} - E^c_{CO_2} \tag{2}$$

$$\begin{cases} E^t_{CO_2} = E_G + E_{CHP} \\ E^c_{CO_2} = E^c_G + E^c_{CHP} \end{cases} \tag{3}$$

Where: C_c represents the carbon trading price; C_μ is the reward coefficient; C_β epresents the growth rate of tiered carbon trading, which is the penalty coefficient, typically set at 0.25; l represents the carbon emission range, typically set at 0.5t; $E^t_{CO_2}$ represents the actual carbon emission of the system, with the unit being t $E^c_{CO_2}$ represents the initial carbon allowance for the system, with the unit being t; ΔE_{CO_2} is the carbon emissions actually participating in the carbon trading market; E_G and E_{CHP} are the actual carbon emissions of thermal power generating units and cogeneration units respectively.

2.2 Green Certificate Market Trading Model

As a certification mechanism validating renewable energy consumption, green certificates mandate a minimum proportion of new energy within the electricity mix, encouraging power retailers and users to adopt green electricity and stimulating renewable energy demand. An operator's green certificate holdings are proportional to its renewable generation. Surplus certificates beyond the regulatory quota can be traded for supplementary income, while deficiencies necessitate market purchases to maintain compliance.The expression of green card quota quantity, green card quantity obtained from renewable energy power generation and green card transaction cost C is shown in (4).

$$\min C_2 = \begin{cases} C_{tgc} = a_0 - b_0(P_{tgc,sell} - P_{tgc,buy}) \\ a_0 = \rho_{tgc} \\ b_0 = (1-v_{tgc})\rho_{tgc} / P_{tgc,sell} \end{cases} \tag{4}$$

Where: C_{tgc} is the transaction price of the green card; a_0 and b_0 are positive parameters of green card market respectively; $P_{tgc,sell}$ and $P_{tgc,buy}$ are the green certificates sold and purchased in the green certificate market respectively; ρ_{tgc} is the basic transaction price of green securities; v_{tgc} is the proportion coefficient of green card price.

The carbon green card trading mechanism is shown in Figure 1.

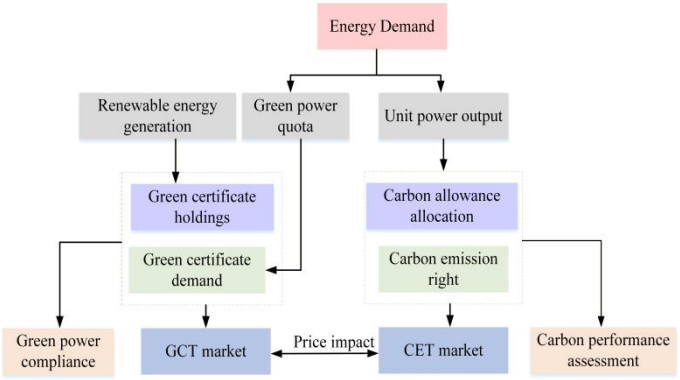

Figure 1 Carbon Green Card Trading Mechanism Chart

3 IES MODEL CONSIDERING GAS HEATING NETWORK

3.1 Gas Inertia Model

The gas network is mainly composed of gas sources, pipelines, compressors and loads, and its structure is shown in Figure 2. Gas inertia describes the pressure, flow changes and gas storage effects in the gas pipeline network, especially the dynamic response of gas flow to pressure and velocity when the load changes suddenly. The gas inertia response equation is described based on mass conservation, momentum conservation, gas state equation, etc., and its model expression is shown in (5).

$$AL\cdot\frac{d^2P_g}{dt^2}+A\lambda vL\cdot\frac{dP_g}{dt}+\frac{A}{L}(P_g-P_0)=-fg-\frac{\lambda v}{2D}g \tag{5}$$

Where: P_0 is the initial pressure of gas; P_g is the outlet pressure of gas pipeline; g is the pipeline gas flow; A is the cross-sectional area of the pipeline; L is the pipe length; λ is the pipeline friction coefficient; v is the flow rate of gas; D is the pipe diameter; f is the item of pipeline friction loss.

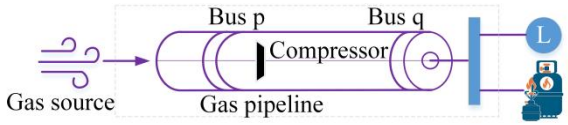

Figure 2 Gas Network Structure

3.2 Thermal Inertia Modeling

Considering the temperature change in the thermal system, especially the lag effect of heat storage and transmission, and based on the heat conservation equation and heat conduction equation, combined with the exponential decay characteristics, the thermal inertia model of the thermal system is established. The model is expressed as (6).

$$T_t=\frac{H_2-H_1}{}+\left(\frac{2H_1-H_2}{}+\frac{\epsilon T_{out}+CMT_0}{CM}\right)e^{-\frac{\epsilon}{CM}t} \tag{4}$$

Where: T_t is the temperature of heating medium at time t; H_1 and H_2 are the input and output thermal power respectively; ϵ is the heat loss coefficient; CM is the heat capacity; T_{out} is the ambient temperature; T_0 is the initial temperature.

The heating network structure is shown in Figure 3.

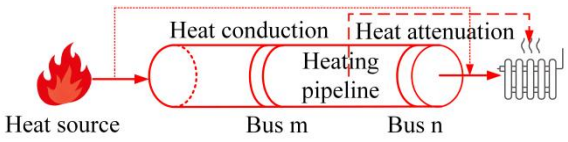

Figure 3 Heating Network Structure

4 LOW CARBON OPTIMAL SCHEDULING MODEL OF IESS CONSIDERING THERMAL INERTIA

4.1 Objective Function

Leveraging the distinct characteristics of gas and thermal inertia, the optimal dispatch of electricity, heat, and gas aims to harness these inertial properties to appropriately coordinate the output of each device, thereby achieving the economic operation of the IES. Consequently, the optimization objective is formulated to minimize the total IES cost,

with the operating cost comprising gas-thermal inertia adjustment costs, energy procurement costs, carbon trading costs, and green certificate costs. The objective function is specifically expressed as (5).

$$\min C = \sum_{T}(C_t^{\text{total}} + C_1 + C_2 + C_t^{\text{inertia}} + C_t^{d}) \tag{5}$$

Where: C_t^{total} is the operating cost of the system at time t; C_t^{inertia} is the power purchase adjustment costof gas thermal inertia at time t; C_t^{d} is the maintenance cost of each device at time t.

4.1.1 System operation cost

The operation cost of the system includes power purchase cost, gas purchase cost, heating cost and energy storage cost, and its expression is shown in (6-9).

$$C_t^{\text{total}} = C_{\text{elec}} + C_{gas} + C_{heat} + C_{storage} \tag{6}$$

$$C_{\text{elec}} = \sum_{t} P_{\text{L}}(t) \cdot C_{\text{elec,unit}} \tag{7}$$

$$C_{\text{gas}} = \sum_{t} F_{\text{gas}}(t) \cdot C_{\text{gas,unit}} \tag{8}$$

$$C_{\text{heat}} = \sum_{t} Q_{\text{heat}}(t) \cdot C_{\text{heat,unit}} \tag{9}$$

Where: C_{elec} is the power purchase cost; C_{gas} is the cost of gas purchase; C_{heat} is the heating cost; $C_{storage}$ is the energy storage cost; $P_{\text{L}}(t)$ is the power load at the moment; $F_{\text{gas}}(t)$ is the gas consumption at time t; $Q_{\text{heat}}(t)$ is the heat supply at time t; $C_{\text{elec,unit}}$ is the unit electricity price; $C_{\text{heat,unit}}$ is the unit gas price; $C_{\text{gas,unit}}$ is the unit heating price.

4.1.2 Cost of gas thermal inertia regulation

The thermal inertia of gas is used to buffer the fluctuation between energy supply and demand and improve system stability, but inertia response takes time, so the scheduling cost is shown in equation (10).

$$C_{\text{inertia}} = \sum_{t}\left(\alpha_{\text{gas}} \cdot \frac{d^2 P_{\text{gas}}}{dt^2} + \alpha_{\text{heat}} \cdot \frac{d^2 T_{\text{heat}}}{dt^2}\right) \tag{10}$$

Where: $\frac{d^2 P_{\text{gas}}}{dt^2}$ is the second derivative of natural gas power; $\frac{d^2 T_{\text{heat}}}{dt^2}$ is the second derivative of heating temperature; α_{gas} and α_{heat} are adjustment cost coefficients respectively.

4.2 Constraint Condition

4.2.1 Power system constraints

The power balance constraint is shown in (11).

$$\begin{cases} P_{PV}^t + P_{WT}^t + P_e^t + P_{GT}^t + P_{ESS,d}^t = P_{load}^t + P_{ESS,c}^t + P_{HP}^t \\ H_{HP}^t + H_{GB}^t + P_{TES,d}^t = H_{load}^t + P_{TES,s}^t \\ Q_{GB}^t + Q_{GT}^t = Q_{gas}^t \end{cases} \tag{11}$$

Where: P_{PV}^t and P_{WT}^t are photovoltaic and wind pow output in t period respectively; P_e^t is the electricity purchase in t period; P_{GT}^t is the output power of GT in t period; Q_{GB}^t and Q_{GT}^t are the gas consumption of GB and GT in t period respectively; P_{load}^t、H_{load}^t and Q_{gas}^t are the electrical loads、heating load and gas load in t period respectively; $P_{TES,d}^t$ is the heat storage boiler power in t period.

4.2.2. Interaction power constraint with the main network.

$$P_{\min}^{buy} \le P_t^{buy} \le P_{\max}^{buy} \tag{12}$$

Where: $P_{\max}^{buy}$ and $P_{\min}^{buy}$ are the maximum and minimum power of power purchase respectively.

5 MODEL SOLVING

This paper proposes an improved Particle Swarm Optimization (PSO) algorithm for solving a low-carbon optimization model of IES that considers gas and thermal inertia. However, when applied to complex power system optimization problems, it often tends to converge to local optima.

To address this limitation, this study introduces improvements in three key aspects. First, an adaptive inertia weight adjustment strategy based on a cosine function is incorporated to dynamically balance the algorithm's global exploration and local exploitation capabilities. Second, in the later stages of iteration, a reverse search strategy is applied to particles identified as locally optimal, enhancing fine-grained search in promising regions. Finally, a stagnation detection and velocity intervention mechanism is designed: if a particle's position continues to update while its fitness value shows no improvement over multiple iterations, its current velocity is reset to the vector sum of its velocities from several

previous iterations, thereby assisting the particle in escaping stagnation. The modified expression for the inertia weight and the corresponding velocity update equation are given in Formula (13-15).

$$\omega_c = (\omega_{\min} + 0.25) + (\omega_{\max} - \omega_{\min} - 0.25) \bullet \cos(\pi(n / N)) \tag{13}$$

$$V_{n,l} = \omega_c V_{n-1,l} + c_1 r_1 (pt_{n-1,l-x_{n-1,l}}) + c_2 r_2 (gt_{n-1,l-x_{n-1,l}}) \tag{14}$$

$$V_{n+1,l} = -\frac{m+2}{m+1}(V_{n,l} + \ldots + V_{n-m+1,l} + V_{n-m,l}) \tag{15}$$

Where: ω_c is the improved inertia weighting factor; $\omega_{\min}$ and $\omega_{\max}$ are the maximum and minimum values of inertia weight coefficient respectively, taking 0.9 and 0.4; N is the number of iterations; $V_{n-1,l}$ and $V_{n,l}$ are the velocities of the L-th particle in the population at the n-1st and n-th iterations; c_1 and c_2 are individual learning factors and group learning factors, respectively; r_1 and r_2 are random numbers uniformly distributed in [0,1], respectively; $pt_{n-1,l-x_{n-1,l}}$ and $gt_{n-1,l-x_{n-1,l}}$ are the historical optimal position and the optimal population position of the L-th particle at the n-th iteration, respectively.

To avoid being trapped in local minima during the search for the optimal solution, a dimension transformation strategy is applied to underperforming particles detected by the self-guidance mechanism, enabling these particles to escape from current poor regions. The corresponding expression is given in Equation (16).

$$Y(l,n) = \frac{\sum_{j=n-q+1}^{n} (f(pt_l(j-1)) - f(pt_l(j)))}{\sum_{j=n-q+1}^{n} (f(gt_l(j-1)) - f(gt_l(j)))} \tag{16}$$

Where: $Y(l,n)$ denotes the ratio of the change in the personal best fitness of the L-th particle to the change in the global best fitness over the preceding q iterations at the n-th iteration; $f(pt_l(j)$ is the variation function of individual optimal fitness in the first Q iterations when the L-th particle is in the nth iteration; $f(gt_l(j)$ is the general optimal individual fitness change function in the first Q iterations when the L-th particle is in the nth iteration; when $Y(l,n)$ is 0 or infinite, it means that the algorithm is currently in a local optimal state. Based on the idea of genetic variation, the positions of the filtered inferior particles and the globally optimal particles are randomly exchanged.The solving steps of the improved particle swarm optimization algorithm are as follows:

Step1: the particle swarm is randomly initialized, i.e., the EO and EU particle swarms are initialized.

Step2: the inertia weight of the particles is adjusted, followed by the calculation of their velocities and the updating of their positions.

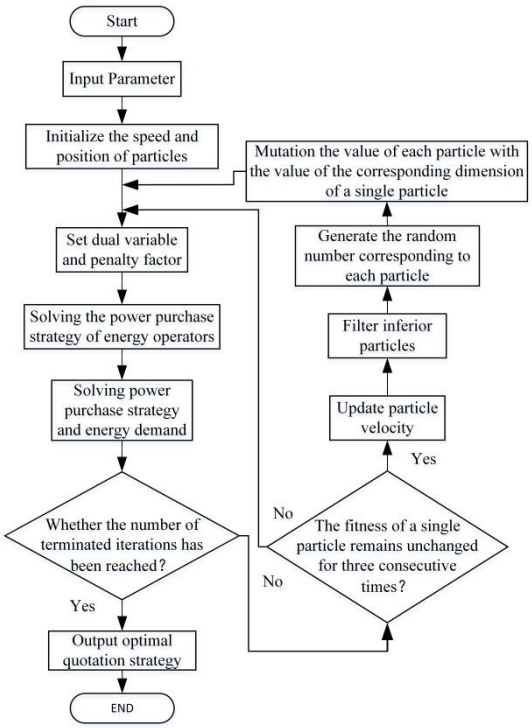

Figure 4 Improved Particle Swarm Algorithm Flowchart

Step3: check whether the swarm's optimal fitness satisfies the predefined iteration accuracy requirement. If yes, output the optimal output strategy and the optimal energy consumption strategy for trading. If not, return to Step 2 and continue the iterative process until the termination condition is met.
The solution procedure is illustrated in Figure 4.

6 CASE STUDY

To reduce system carbon emissions and promote renewable energy utilization, this paper investigates a low-carbon optimal dispatch strategy for an IES considering gas and thermal inertia. A power system from a region with a high penetration of renewable energy is adopted for data simulation, in which the capacity of the thermal power generating unit is 660 MW, while the capacities of the wind and photovoltaic generating units are 300 MW each. The forecasted output profiles of renewable energy sources are shown in Figure 5.

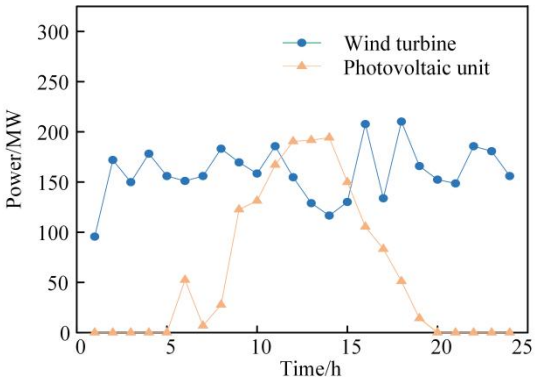

Figure 5 Predicted Power for Renewable Energy

As shown in Figure 6, during the period from 0:00 to 5:00, wind turbines provide a relatively high output, while between 10:00 and 14:00, the output of photovoltaic units reaches its peak.
The electricity market price curve is shown in Figure 7.

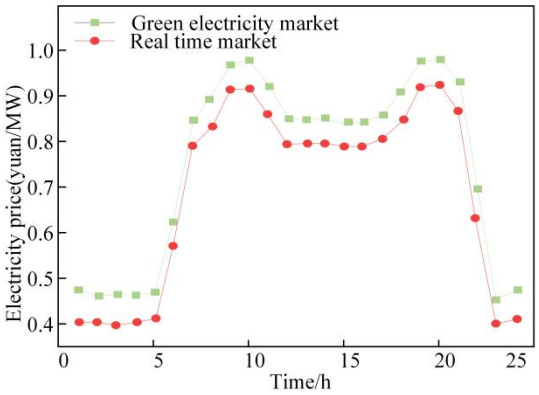

Figure 6 Electricity Market Price Curve

To mitigate system carbon emissions and enhance renewable energy utilization, this paper investigates a low-carbon optimal dispatch strategy for an IES that incorporates gas and thermal inertia.

6.1 GET-CET Optimization Analysis

To verify the impact of CET and GCT on the system cost, four operational scenarios are established in this paper:
S1: Optimal operation strategy of a typical IES (without CET or GCT).
S2: Optimal operation strategy of an IES considering only the CET mechanism.
S3: Optimal operation strategy of an IES considering only the GCT mechanism.
S4: Optimal operation strategy of an IES considering both CET and GCT mechanisms

Table 1 System Costs under Different Scenarios

case	Operating cost/yuan	CET(yuan/kg)	GCT(yuan/kg)	Total cost /yuan
S1	83651.1	0	0	83651.1
S2	83650.1	8717.0	0	74933.1

S3	85365.8	0	11098.0	74267.8
S4	84529.4	8812.1	10112.4	65604.7

Table 1 presents the system costs under the four scenarios. It can be observed that Scenario 4 achieves the lowest total system cost. Compared to Scenario 1, the system cost is reduced by 21.57%. Relative to Scenario 2, which only considers the CET mechanism, the system cost decreases by 10.42%. In comparison with Scenario 3, which solely incorporates the GCT mechanism, the system cost is lowered by 11.22%. This improvement can be attributed to the synergistic effect of simultaneously implementing CET and GCT. On one hand, the system tightens carbon emission constraints, thereby increasing revenue from carbon emissions trading. On the other hand, it enhances the integration of renewable energy, enabling the acquisition of additional revenue from green certificate trading. Consequently, the concurrent adoption of carbon emissions trading and green certificate trading mechanisms improves the economic efficiency of system operation.
Figure 7 illustrates the clearing price variation curve in the electricity market under the coupled implementation of CET and GCT.

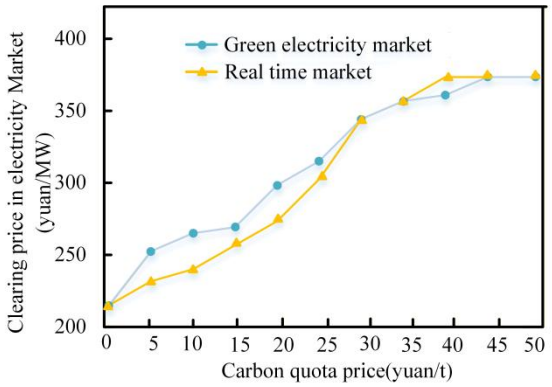

Figure 7 The Clearing Price Curve of the Electricity Market

As illustrated in Figure 7, when carbon allowances are slightly tightened, the increase in electricity market prices remains limited, and high-emission power plants tend to inflate their costs. In the case of a substantial reduction in carbon allowances, even low-emission power plants are required to purchase emission rights, whereas the profits of high-emission plants may be insufficient to cover such costs. Under these circumstances, all traditional energy power generation enterprises are likely to bid at costs higher than their actual levels, leading to a significant rise in electricity prices. Conversely, if carbon allowances are relatively loose, the carbon market imposes fewer restrictions on power generation, and low carbon prices exert no notable impact on bidding behavior. However, when carbon prices are high, energy operators tend to engage in carbon market trading and submit high-cost bids in the electricity market to capture profits, thereby driving a sharp increase in electricity prices.

6.1 Gas-Thermal Inertia Effects

To investigate the impact of gas-thermal inertia on the optimal scheduling of the system, four operational modes are established, as outlined below:
Scenario 1: Traditional optimization strategy without considering thermal inertia;
Scenario 2: Optimization strategy considering only thermal inertia;
Scenario 3: Optimization strategy considering only gas inertia;
Scenario 4: Optimization strategy considering both gas and thermal inertia.
The system operating costs under each strategy are presented in Table 2.

Table 2 System Operating Costs under Different Strategies

Scenario	Energy inertia	Total cost/kCNY
Scenario 1	Without inertia	296.35
Scenario 2	Thermal inertia	293.56
Scenario 3	Gas inertia	292.16
Scenario 4	Gas and thermal inertia	291.20

Scenario 1 disregards gas-thermal inertia, employing a traditional direct-electric heating boiler for real-time energy balance and maintaining constant indoor temperature; thus, unit output closely follows load variations.
Scenario 2 considers only thermal inertia, resulting in lower heating output than Scenario 1 and reduced overall cost. As shown in Figure 8, Scenario 4 exhibits a hysteresis in the heating output of the CHP unit, attributed solely to the

transmission thermal inertia of the heating network, which enables partial heat storage in pipelines and leverages the energy storage characteristic of the heating network.

Scenario 3 considers only gas inertia. As illustrated in Figure 8, due to the relatively stable variations in gas and heat loads, the pipeline storage capacity of the gas network is primarily influenced by changes in electrical load. During the periods of 07:00–09:00 and 16:00–17:00, when electrical load demand is relatively low, natural gas is stored and subsequently released during periods of high demand. This approach mitigates the constraint of gas supply capacity on gas output, thereby enhancing the flexibility and reliability of system operation.

Scenario 4 incorporates both thermal inertia and gas inertia. Figure 9 clearly demonstrates that during the period of 10:00–21:00, when electrical load demand is relatively high, the combined heat and power (CHP) unit in Scenario 4 generates more output compared to Scenario 3, with a total heating power 1.2 times that of Scenario 3. This is because, relative to Scenario 3, which only considers gas inertia, Scenario 4, which additionally accounts for thermal inertia, enables the preferential dispatch of CHP units with superior economic performance. The thermal energy generated by the CHP unit can be stored in the pipelines of the heating network and within buildings for flexible dispatch. Consequently, Scenario 4, which comprehensively considers both thermal inertia and gas inertia, achieves the lowest total operating cost.

In summary, the refined modeling of energy inertia within natural gas and thermal systems enables the utilization of distinct inertial characteristics, thereby fully leveraging the energy storage capabilities of both the gas network and heating network to achieve economically optimal system operation.

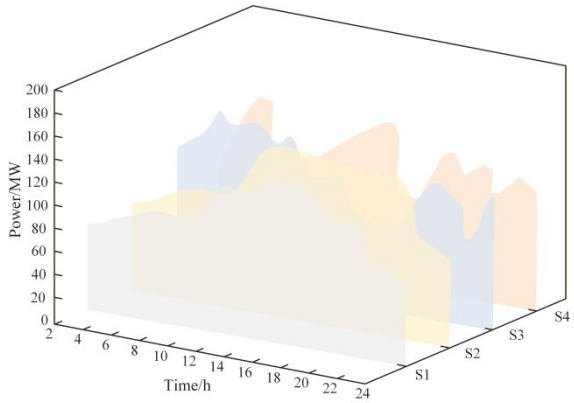

Figure 8 Heating Power Output of the CHP Unit in Different Periods

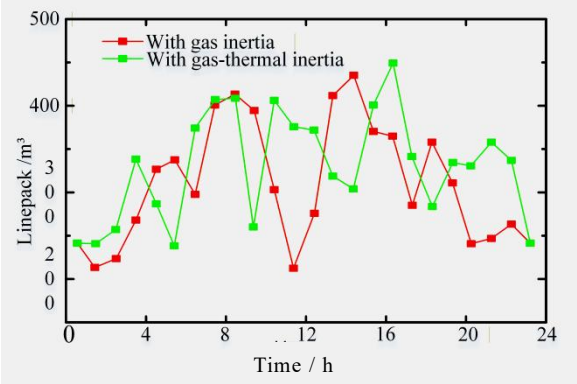

Figure 9 Total Gas Storage Variation

7 CONCLUSION

Addressing the low-carbon economic dispatch problem of an IES, this paper proposes a low-carbon optimal scheduling strategy that incorporates gas-thermal inertia, achieving a synergistic improvement in system economic efficiency and renewable energy accommodation. The main conclusions are as follows:

(1) Based on the dynamic characteristics of the natural gas network, a gas inertia model is developed to describe variations in pressure, flow rate, and pipeline storage. Concurrently, considering the transmission delay and energy storage characteristics of the district heating system, a dynamic equation for thermal inertia is formulated to quantify heat loss and time lag, providing a theoretical foundation for the refined dispatch of multi-energy coupling systems.

(2) The coordinated utilization of gas-thermal inertia effectively leverages the energy storage potential of both the natural gas network and the heating system. Case study results demonstrate that, compared to traditional strategies without considering inertia, the proposed approach reduces the total system cost to 291,200 CNY, validating its effectiveness in enhancing system flexibility and economic performance.

(3) Building upon the gas-thermal inertia scheduling framework, the introduction of CET and GCT mechanisms further reduces the total system cost and significantly improves the renewable energy accommodation rate. This indicates that the integration of low-carbon market mechanisms with energy inertia constitutes an effective pathway for promoting the low-carbon economic operation of IES.

Future research can further investigate issues such as uncertainty and multi-timescale optimization to enhance the robustness and engineering applicability of the proposed strategy.

COMPETING INTERESTS

The authors have no relevant financial or non-financial interests to disclose.

REFERENCES

[1] Huang X. The multidimensional relationship between renewable energy deployment and carbon dioxide emissions in high-income nations. npj Climate Action, 2024, 3(1): 107.

[2] Adebayo T S, Uhunamure S E, Shale K. A time-varying approach to the nexus between environmental related technologies, renewable energy consumption and environmental sustainability in South Africa. Scientific Reports, 2023, 13(1): 4860.

[3] Wang X, Zhang Z, Liu C, et al. Analysis of renewable energy absorption and economic feasibility in multi-energy complementary systems under spot market conditions. Energy Engineering: Journal of the Association of Energy Engineers, 2025, 122(2): 577.

[4] Luo Z, Liu H Z, Zhao W J, et al. Optimization of collaborative operation of cross-border integrated energy system considering carbon trading-green certificate joint trading. Electric Power Automation Equipment, 2023, 43(11): 1-8+25.

[5] Zhang H T, Zhou Y J, Yan L Y, et al. Multi-time scale optimal scheduling of integrated energy system considering green certificate-carbon trading and hydrogen energy. Journal of Electric Power System and Automation, 2023, 35(11): 95-106.

[6] Zhang H, Meng Q Y, Wang M C, et al. Economic low-carbon dispatching strategy of hydrogen-containing integrated energy system considering the participation of thermal power units in green certificate purchase transaction. Power System Protection and Control, 2023, 51(3): 26-35.

[7] Liang Z, Ma Z C, Wei Z B, et al. Operation optimization and decision analysis of CSP generators in electric-thermal integrated energy market. Electric Power Automation Equipment, 2022, 42(12): 9-16.

[8] Zhang L, Liu D, Cai G, et al. An optimal dispatch model for virtual power plant that incorporates carbon trading and green certificate trading. International Journal of Electrical Power & Energy Systems, 2023, 144: 108558.

[9] Ma N, Fan L. Double recovery strategy of carbon for coal-to-power based on a multi-energy system with tradable green certificates. Energy, 2023, 273: 127270.

[10] Sun P, Teng Y, Leng O Y, et al. Coordinated optimization of electric-thermal integrated system considering multiple thermal inertias of heating system. Proceedings of the CSEE, 2020, 40(19): 6059-6071.

[11] Yao S, Gu W, Zhang X S, et al. Effect of heating network characteristics on ultra-short-term scheduling of integrated energy system. Automation of Electric Power Systems, 2018, 42(14): 83-90.

[12] Xu J, Hu J, Liao S Y, et al. Cooperative optimization of integrated energy system considering dynamic characteristics of network and integrated demand response. Automation of Electric Power Systems, 2021, 45(12): 40-48.

[13] Ordoudis C, Delikaraoglou S, Kazempour J, et al. Market-based coordination of integrated electricity and natural gas systems under uncertain supply. European Journal of Operational Research, 2020, 287(1): 110-119.